

Coupling to spin fluctuations from conductivity scattering rates

E. Schachinger¹ and J. P. Carbotte²

¹*Institut für Theoretische Physik, Technische Universität Graz, A-8010 Graz, Austria*

²*Department of Physics and Astronomy, McMaster University, Hamilton, Ontario, Canada L8S 4M1*

(Received 12 June 2000)

A recent analysis of optical conductivity data which has provided evidence for coupling of the charge carriers to the 41-meV spin resonance seen in the superconducting state of optimally doped YBa₂Cu₃O_{6.95} (Y123) is extended to other systems. We find that the corresponding spin resonance is considerably broader in Tl₂Sr₂CuO_{8+δ} (Tl2201) and YBa₂Cu₄O₈ (Y124) than it is in Bi₂Sr₂CaCu₂O_{8+δ} (Bi2212) and there is no resonance in overdoped Tl2201 with $T_c = 23$ K. The effective charge-spin spectral density is temperature dependent and contains feedback effects that further stabilize superconductivity as T is reduced.

For a conventional electron-phonon system an isotropic, on the Fermi surface, spectral density can be introduced which is essentially temperature independent below T_c .¹ This spectral density, $\alpha^2F(\omega)$, can be determined from tunneling data in the superconducting state and has been used with great success to understand the deviations from BCS universal laws observed in many conventional superconductors.¹ In principle, information on $\alpha^2F(\omega)$ can also be obtained through inversion of optical data although, to our knowledge, this has only been accomplished for Pb.²

Recently Marsiglio *et al.*³ introduced a dimensionless function $W(\omega)$ which is defined as the second derivative of the normal-state optical scattering rate $\tau^{-1}(\omega) = (\Omega_p^2/4\pi)\text{Re } e\sigma_N^{-1}(\omega)$ multiplied by frequency ω . Here Ω_p is the plasma frequency and $\sigma_N(\omega)$ the normal state optical conductivity. Specifically,

$$W(\omega) = \frac{1}{2\pi} \frac{d^2}{d\omega^2} \left[\frac{\omega}{\tau(\omega)} \right] \quad (1)$$

which follows directly from experiment, provided the data on $\sigma_N(\omega)$ are sufficiently accurate that a meaningful second derivative can be taken, possibly after smoothing. Marsiglio *et al.*³ made the very important observation that within the phonon range $W(\omega) \approx \alpha^2F(\omega)$ at least for those spectral densities studied. Beyond the phonon range $W(\omega)$ can be negative but this does not distract from the fact that $W(\omega)$ can be used to get the shape and magnitude of $\alpha^2F(\omega)$. Application of Eq. (1) to the normal-state conductivity of K₃C₆₀ gave an $\alpha^2F(\omega)$ [provided negative regions in $W(\omega)$ are simply ignored] in excellent agreement with incoherent inelastic neutron-scattering data^{4,5} on the phonon frequency distribution $F(\omega)$ and gave sufficient coupling strength to obtain the measured value of T_c . This leaves little doubt that K₃C₆₀ is an s -wave, electron-phonon superconductor, even though correlation effects are likely to be quite important.⁵

More recently Carbotte *et al.*⁶ have extended the method of Ref. 3 to spin-fluctuation exchange systems and to the superconducting state with d -wave symmetry. The charge carriers are coupled to the spin fluctuations through the spin susceptibility which is strongly peaked at (π, π) in the two-dimensional Brillouin zone of the CuO₂ plane of the high- T_c oxides.⁷ In this case the momentum dependence of the inter-

action is very important and cannot be pinned to the Fermi surface⁸ and there are cold and hot spots. Nevertheless, the resulting in-plane infrared conductivity is isotropic for tetragonal systems and Eq. (1) can still be applied and the resulting $W(\omega)$ interpreted as an effective spectral density for the electron-spin fluctuation exchange interaction.⁹ In contrast to the electron-phonon case this effective interaction resides in the system of electrons and, due to correlation effects, can be temperature dependent. In particular, it can undergo major changes when the electrons condense into the superconducting state. Such feedback effects are generic to any electronic mechanism.¹⁰⁻¹² They have been studied theoretically within a Hubbard model by Dahm and Tewordt¹³ who also review the work of others.

Optical conductivity calculations for a d -wave superconductor^{12,14} within a spin-fluctuation mechanism by Carbotte *et al.*⁶ established that $W(\omega)$ of Eq. (1) still gives a good approximation to the spectral density $I^2\chi(\omega)$ provided it is divided by 2 and shifted by the gap Δ_0 . Calculations of $W(\omega)$ from the data of Basov *et al.*¹⁵ in optimally doped Y123, revealed strong coupling of the charge carriers to the 41-meV spin resonance seen below T_c in spin polarized inelastic neutron-scattering experiments.^{16,17} The coupling to this resonance was found to be large enough to stabilize the observed superconducting state. For underdoped Y123 the spin resonance remains in the optics even above T_c up to a pseudogap temperature, in agreement with the neutron work by Dai *et al.*¹⁸ A quantitative analysis is not attempted in this case, however, because of the added complications of the pseudogap.

Here we extend our previous work⁶ to other materials and, in contrast to what was done in Ref. 6, we proceed here without any reference to neutron data. In Fig. 1 we show results for the coupling to the spin resonance in Y124 ($T_c = 82$ K, solid line), Tl2201 ($T_c = 90$ K, dashed line), and Bi2212 ($T_c = 90$ K, dotted line) derived from optical data measured at $T = 10$ K. These results were obtained from a direct application of Eq. (1) to the optical data of Puchkov *et al.*¹⁹ Shifting by the gap which is determined by the method discussed in detail later on, the resonances are at 38, 43,²⁰ and 46 meV, respectively with a considerably larger width in the first two than in Bi2212. On the other hand, the spin resonance in Bi2212 was observed by Fong *et al.*²¹ at

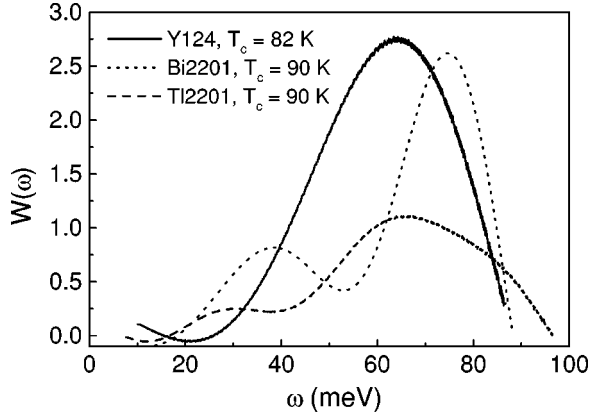


FIG. 1. The spin resonance obtained from inversion of (supercond.) optical conductivity data using Eq. (1) for $W(\omega)$: solid line Y124 ($T_c=82$ K), dashed TI2201 ($T_c=90$ K), and dotted Bi2201 ($T_c=90$ K). Note that the vertical scale is dimensionless. The position of the resonance peak is shifted by the gap value on the horizontal scale.

43 meV using neutron scattering. No neutron data exist, to our knowledge, for Y124 and TI2201 and therefore our results represent a falsifiable prediction. Another prediction that we develop later is that overdoped TI2201 ($T_c=23$ K) will show no resonance.

To extract more information from optical data we need to consider a more specific mechanism, namely spin-fluctuation exchange.^{7,22} At the simplest level in the normal state, we describe the corresponding spectral density by a two parameter form

$$I^2\chi(\omega) = I^2 \frac{\omega\omega_{SF}}{\omega^2 + \omega_{SF}^2}, \quad (2)$$

where I^2 is the coupling between spin excitations and the charge carriers and ω_{SF} sets the energy scale for the spin fluctuations. Both parameters can be derived from a fit to the normal-state optical scattering rates as a function of frequency. A fit for TI2201 ($T_c=90$ K) is shown in the top frame of Fig. 2. The fit to the $T=300$ -K data with $\omega_{SF}=100$ meV and a high-energy cutoff at 400 meV is excellent and lowering ω_{SF} to 30 meV does not give an acceptable fit. The formalism we use to relate spectral density to conductivity is standard³ and $\sigma_N(\omega)$ follows from a knowledge of the self-energy $\Sigma(\omega)$. As a check on the accuracy of the inversion procedure embodied in Eq. (1), we show in the central frame of Fig. 2 our results for the function $W(\omega)$ obtained from our theoretical normal-state optical scattering rate $\tau^{-1}(\omega)$ based on our input spectral density $I^2\chi(\omega)$ given in Eq. (2) and shown as the grayed squares. We see, that at $T=10$ K the inversion matches almost perfectly the input spectral density except for small wiggles in the inverted curve (solid line). This excellent agreement between $W(\omega)$ and $I^2\chi(\omega)$ is not limited to simple, smooth forms. In the bottom frame of Fig. 2 we show results obtained for a structured spectrum, namely a spectrum which is proportional to the one used by Schachinger and Carbotte²⁰ to analyze the optical properties of superconducting TI2201. Ex-

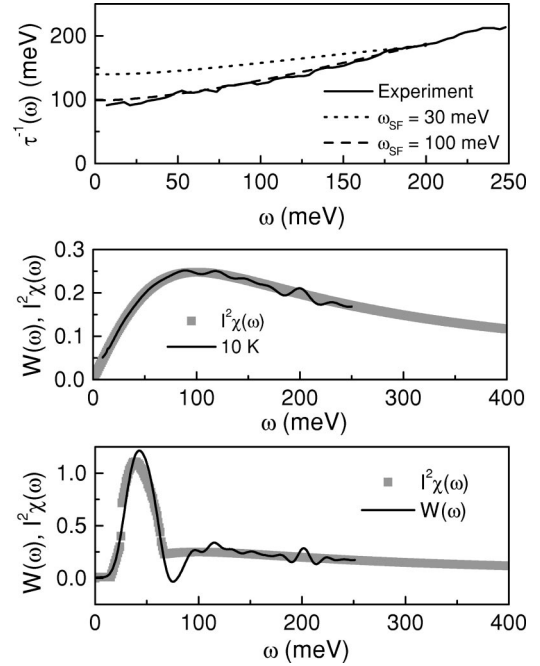


FIG. 2. The top frame gives the optical scattering rate at $T=300$ K in the normal state of TI2201 ($T_c=90$ K). The solid curve is experiments, the dashed one a fit with $\omega_{SF}=100$ meV in Eq. (2), and the dotted line is for $\omega_{SF}=30$ meV. The middle frame gives the input $I^2\chi(\omega)$ (grayed solid squares) used in the conductivity calculations which give $W(\omega)$ (solid line) at $T=10$ K. The bottom frame gives another model for $I^2\chi(\omega)$ based on TI2201 (grayed solid squares) and the corresponding $W(\omega)$ at $T=10$ K.

cept for some oscillations at higher frequencies the normal state $W(\omega)$ (solid curve) is close to the input spectral function $I^2\chi(\omega)$ (grayed squares).

Normal-state conductivity data are not available at low temperatures in the high- T_c oxides and it is necessary to devise an inversion technique which applies in the superconducting state. Also, the spectral density can depend on temperature and on the state of the system. This requires a formalism which relates the spectral density $I^2\chi(\omega)$ to the superconducting state conductivity. This was provided in the work of Schachinger *et al.*¹² who calculated the conductivity of a d -wave superconductor within an Eliashberg formalism. As previously stated, using this formalism Carbotte *et al.*⁶ established that in this case $W(\omega)/2$ agrees fairly well with $I^2\chi(\omega)$ provided it is shifted by the gap amplitude Δ_0 . This is shown clearly in Fig. 3 which is similar to the bottom frame of Fig. 2 except that now the superconducting state conductivity has been employed and the material is Bi2201 with $T_c=90$ K rather than TI2201. The grayed squares are the input spectral density shifted by the theoretical gap $\Delta_0=28$ meV and the dashed line are the results for the inversion $W(\omega)/2$ vs ω based on the calculated $\sigma_S(\omega)$. A simple d -wave gap model was used, and a parameter g introduced giving the relative weight of the spin-fluctuation spectral density in the gap channel as compared to its value in the renormalization channel. Details can be found in Ref. 12. For Bi2201, $g=0.725$, gives the measured value of T_c when the normal-state spectral density of Eq. (2) is used in the linearized self-energy equations at $T=T_c=90$ K. This value of g , which is considerably less than 1, could be interpreted as an

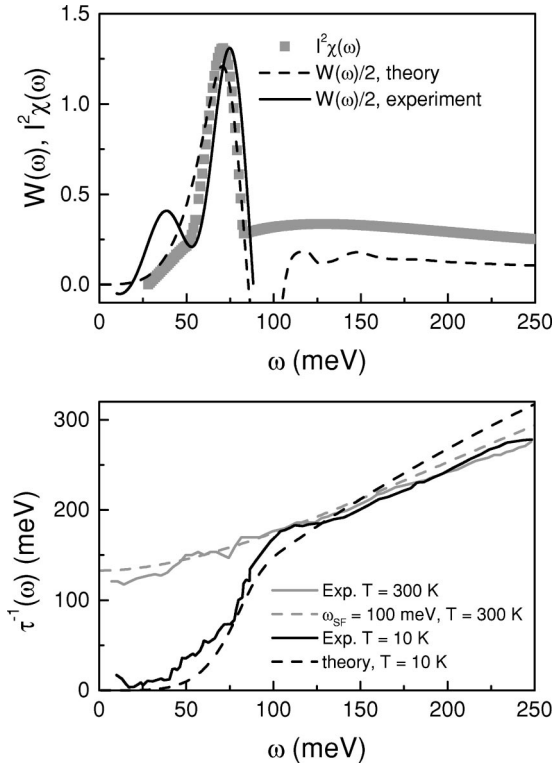


FIG. 3. The top frame gives our model for the spin-fluctuation spectral density (displaced by the theoretical gap $\Delta_0=28$ meV) for Bi2212 in the superconducting state at $T=10$ K (grayed solid squares). The dashed line is $W(\omega)/2$ obtained from the calculated conductivity and the solid line is the resonant peak of Fig. 1 (dotted line) used in constructing the model $I^2\chi(\omega)$. The bottom frame shows two sets of optical scattering rates and theoretical fits to these. The solid lines are experimental and the dashed lines are the theoretical results. The grayed lines are for the normal state at $T=300$ K and the black ones are for the superconducting state at $T=10$ K.

indication that a second, subdominant scattering mechanism (for example phonons) is also operative. The theoretical gap, on the other hand, is calculated from the solution of the d -wave Eliashberg equations¹² for a temperature $T=10$ K and is defined as the peak in the quasiparticle density of states. It is to be noted that this gap is a bit smaller than the gap of 31 meV suggested from the inversion data of Fig. 1 for Bi2212 (dotted line) using the experimentally observed position of the resonance peak at 43 meV.²¹ Nevertheless, the agreement is excellent and the theoretical value of 28 meV is within the experimentally observed range.²³

The agreement between $W(\omega)/2$ and $I^2\chi(\omega)$ in the top frame of Fig. 3 as to size and shape of the main peak is excellent. However, a negative piece is introduced in $W(\omega)$ right above the spin resonance peak which is not part of the spectral density. Nevertheless, at higher energies, $W(\omega)/2$ does recover and shows long tails extending to several 100 meV although they are underestimated. Additional evidence for the existence of this high-energy background is found from our fit to the normal-state data shown in the bottom frame of Fig. 3. The grayed lines give the optical scattering rate in Bi2212 at $T=300$ K. The dashed curve is the fit to this data (solid line) and gives a normal-state spin-fluctuation frequency $\omega_{SF}=100$ meV in Eq. (2) and an area

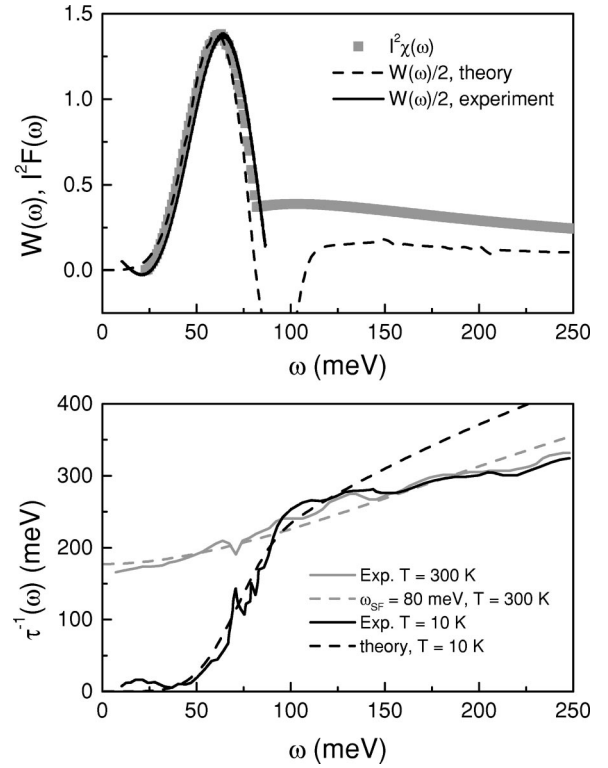


FIG. 4. The same as Fig. 3 but for the material Y124. The spin-fluctuation spectral density $I^2\chi(\omega)$ was displaced by the theoretical gap $\Delta_0=24$ meV in the top frame.

under $I^2\chi(\omega)$ of 95 meV. From application of Eq. (1) to the superconducting state data we have already established the existence of coupling of charge carriers to a resonance peak as seen in Fig. 1 which gives its size and position in energy and this is reproduced as the solid curve in the top frame of Fig. 3. To get the superconducting state spectral density (grayed squares of the top frame in Fig. 3) the low-frequency part of the normal-state response is replaced by the resonant peak.

There is no known sum rule on the spectral weight $I^2\chi(\omega)$ and we find that the area under this function increases from 95 meV in the normal state to 115 meV in the superconducting state. The increase is due to the appearance of the spin resonance. Part of this spectral weight could come from a transfer from higher energies but our resolution at such energies is not sufficient to confirm this. In the bottom frame of Fig. 3 we show the fit to the superconducting state optical scattering rate obtained from our model $I^2\chi(\omega)$. The agreement is very good and since no new parameters were introduced to obtain the black dashed curve which agrees remarkably well with the black solid curve in the region $0 \leq \omega \leq 250$ meV, this is taken to be a strong consistency check on our work.

We extend our analysis to the material Y124 ($T_c=81$ K) where we predict from Fig. 1 a spin resonance to exist at 38 meV. Moreover, this spin resonance is much broader than the one observed in Bi2212 of Y123. Results are presented in Fig. 4. The top frame of this figure demonstrates the agreement between $W(\omega)/2$ and $I^2\chi(\omega)$ which was shifted by the theoretical gap $\Delta_0=24$ meV which is another prediction of our calculations as, to our knowledge, no experimental data exist for this material. The bottom frame

of Fig. 4 presents our comparison between experimental and theoretical optical scattering rates. As in the case of Bi2212 the normal-state scattering rate (grayed lines) at $T=300$ K gives evidence for the existence of a high-energy background as the experimental data (solid line) are best fit by a spin-fluctuation spectrum of the type described by Eq. (2) with $\omega_{SF}=80$ meV and a high-energy cutoff of 400 meV (dashed line). The black lines compare the theoretical results (dashed line) to experiment (solid line) in the superconducting state at $T=10$ K. The signature of the spin resonance, the sharp rise in $\tau^{-1}(\omega)$ starting around 50 meV, is correctly reproduced by theory. For $\omega>120$ meV the experimental scattering rate shows only a weak energy dependence and the theoretical prediction starts to deviate from experiment. This is in contrast to our results for Bi2212 (bottom frame of Fig. 3) and Tl2201,²⁰ and could be related to the fact that the Y124 sample used by Puchkov *et al.*¹⁹ was slightly underdoped, a situation not covered by our theory.

To conclude, we obtained theoretical gap amplitudes $\Delta_0 = 24, 26$, and 28 meV for Y124, Tl2201,²⁰ and Bi2212, respectively. Experimental values are in the range of 30 meV for Bi2212 and 28 meV for Tl2201.²³ The theoretical values correspond to ratios $2\Delta_0/k_B T_c$ of 6.8, 6.7, and 7.2, much larger than the BCS value of ~ 4.3 , and proves that feedback effects, not present in BCS, stabilize the superconducting state as T is reduced (a result also supported by the theoretical study of Dahm and Tewordt¹³).

Next we consider the case of overdoped Tl2201 with $T_c = 23$ K. The data of Puchkov *et al.*¹⁹ are reproduced as the solid curves of Fig. 5. The grayed curves are at $T=300$ K in the normal state and the black curves apply to the superconducting state at $T=10$ K. Nowhere is there a large rapid rise in the $T=10$ K curve at an energy which would correspond to the sum of Δ_0 plus some resonant frequency. This is in striking contrast to the sharp rise seen in Bi2212 and Y124 (bottom frame of Figs. 3 and 4 solid curves). For this overdoped sample no spin resonance forms. In fact, a fit of Eq. (2) with $\omega_{SF}=300$ meV to the $T=300$ K data which gives the grayed dashed curve in good agreement with the data (grayed, solid line) also gives the black dashed curve when used in a superconducting state calculation. The agreement with the solid black curve is quite good. No adjustment of any kind was made. Finally, we note in passing that $\tau^{-1}(\omega)$ stays finite (but very small) in the limit $\omega \rightarrow 0$ in all calculations presented here.

Optical conductivity data in Bi2212, Y124, and Tl2201 (Ref. 20) indicate that in the superconducting state the charge carriers are strongly coupled to a spin resonance

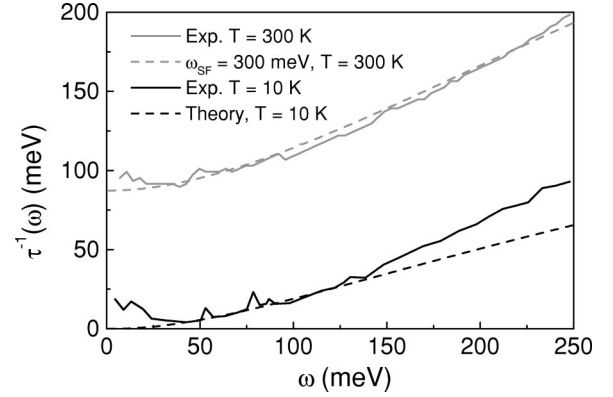


FIG. 5. The optical scattering rates in an overdoped sample of Tl2201 with a $T_c = 23$ K. The solid lines represent the experimental data and the dashed lines fits. The grayed curves apply in the normal state at $T=300$ K and the black curves in the superconducting state at $T=10$ K. No spin resonant peak is found in this case in contrast to the three cases shown in Fig. 1.

which forms only in this state. No such resonance is seen in overdoped Tl2201 with $T_c = 23$ K. These results confirm that the coupling to the spin resonance first seen in optimally doped Y123 is a general feature of several, but not all the high- T_c oxides. The feature that corresponds to the resonance is a sharp rise in the optical scattering rate at a frequency equal to the sum of the gap plus the spin-resonance frequency. Inversion of the optical data gives information on the absolute strength of the coupling between charge carriers and the spin resonance, and on its width. The resonance is found to be considerably broader in Tl2201 and Y124 than it is in Bi2212. In the systems considered here, at T_c , there is only coupling to the background spin fluctuations which extend to high energies. Below T_c a spin resonance forms¹⁸ at low ω and this leads to increased coupling to the spin degrees of freedom which further stabilizes the superconducting state. This feedback effect leads to a ratio of twice the gap to T_c of order 6–8, much larger than the value predicted in weak coupling BCS for a d -wave gap (~ 4.3). Overdoped Tl2201 with $T_c = 23$ K provides an example for which no spin resonance forms below T_c , and this system has optical properties close to those expected for a Fermi liquid.

Research was supported in part by NSERC (Natural Sciences and Engineering Research Council of Canada) and by CIAR (Canadian Institute for Advanced Research). We thank D. N. Basov for continued interest in this work and discussions.

¹J.P. Carbotte, Rev. Mod. Phys. **62**, 1027 (1990).

²B. Farnworth and T. Timusk, Phys. Rev. B **10**, 2799 (1974); **14**, 5119 (1976).

³F. Marsiglio, T. Startseva, and J.P. Carbotte, Phys. Lett. A **245**, 172 (1998).

⁴L. Pintschovius, Rep. Prog. Phys. **57**, 473 (1996).

⁵O. Gunnarsson, Rev. Mod. Phys. **69**, 575 (1997).

⁶J.P. Carbotte, E. Schachinger, and D.N. Basov, Nature (London) **401**, 354 (1999).

⁷P. Monthoux and D. Pines, Phys. Rev. B **47**, 6069 (1993).

⁸D.W. Branch and J.P. Carbotte, Can. J. Phys. **17**, 531 (1999).

⁹D.W. Branch and J.P. Carbotte, J. Supercond. **12**, 667 (1999).

¹⁰D.A. Bonn, P. Dosanjh, R. Liang, and W.N. Hardy, Phys. Rev. Lett. **68**, 2390 (1992).

¹¹M.C. Nuss, P.M. Mankiewich, M.L. O'Malley, and E.H. Westwick, Phys. Rev. Lett. **66**, 3305 (1991).

¹²E. Schachinger, J.P. Carbotte, and F. Marsiglio, Phys. Rev. B **56**, 2738 (1997).

- ¹³T. Dahm and L. Tewordt, Phys. Rev. B **52**, 1297 (1995).
- ¹⁴D. Munzar, C. Bernhard, and M. Cardona, Physica C **312**, 121 (1999).
- ¹⁵D.N. Basov, R. Liang, B. Dabrovski, D.A. Bonn, W.N. Hardy, and T. Timusk, Phys. Rev. Lett. **77**, 4090 (1996).
- ¹⁶J. Rossat-Mignion, L.P. Regnault, P. Bourges, P. Burllet, C. Vettier, and J.Y. Henry, Physica B **192**, 109 (1993).
- ¹⁷Ph. Bourges, Y. Sidis, H.F. Fong, B. Keimer, L.P. Regnault, J. Bossy, A.S. Ivanov, D.L. Milius, and I.A. Aksay, in *High Temperature Superconductivity*, edited by S.E. Barnes, J. Ashkenazi, J.L. Cohn, and F. Zuo, AIP Conf. Proc. **483** (AIP, Woodbury, New York, 1999), pp. 207-212.
- ¹⁸P. Dai, H.A. Mook, S.M. Hayden, G. Aeppli, T.G. Perring, R.D. Hunt, and F. Doğan, Science **284**, 1344 (1999).
- ¹⁹A. Puchkov, D.N. Basov, and T. Timusk, J. Phys.: Condens. Matter **8**, 10 049 (1996).
- ²⁰E. Schachinger and J.P. Carbotte, in: *Proceedings of the 6th International Conference on Materials and Mechanism of Superconductivity and High Temperature Superconductors* [Physica C (to be published)].
- ²¹H.F. Fong, P. Bourges, Y. Sidis, L.P. Regnault, A. Ivanov, G.D. Gull, N. Koshizuka, and B. Keimer, Nature (London) **389**, 588 (1999).
- ²²A.D. Millis, H. Monien, and D. Pines, Phys. Rev. B **42**, 167 (1990).
- ²³T. Hasegawa, H. Ikuta, and K. Kitazawa, in *Physical Properties of High Temperature Superconductors III*, edited by D.M. Ginsberg (World Scientific, Singapore, 1992).